AIP Journal of Applied Physics

Reception of longitudinal vector potential radiation with a plasma antenna

Robert K. Zimmerman

Citation: J. Appl. Phys. **114**, 044907 (2013); doi: 10.1063/1.4816100
View online: http://dx.doi.org/10.1063/1.4816100
View Table of Contents: http://jap.aip.org/resource/1/JAPIAU/v114/i4
Published by the AIP Publishing LLC.

Additional information on J. Appl. Phys.

Journal Homepage: http://jap.aip.org/
Journal Information: http://jap.aip.org/about/about_the_journal
Top downloads: http://jap.aip.org/features/most_downloaded
Information for Authors: http://jap.aip.org/authors

ADVERTISEMENT

Downloaded 27 Aug 2013 to 128.183.169.235. This article is copyrighted as indicated in the abstract. Reuse of AIP content is subject to the terms at: http://jap.aip.org/about/rights_and_permissions

JOURNAL OF APPLIED PHYSICS **114**, 044907 (2013)

Reception of longitudinal vector potential radiation with a plasma antenna

Robert K. Zimmerman, Jr.[a)]
Sigma Space Corporation, NASA Goddard Space Flight Center, 8800 Greenbelt Road, Greenbelt, Maryland 20771, USA

(Received 9 April 2013; accepted 3 July 2013; published online 30 July 2013)

To help resolve the long-running debate between physicists and engineers regarding the existence of the magnetic vector potential, herewith we describe an experiment demonstrating reception of time-harmonic vector potential radiation at 1.3 GHz. © *2013 AIP Publishing LLC*. [http://dx.doi.org/10.1063/1.4816100]

I. INTRODUCTION

For many years the debate has continued as to whether the magnetic vector potential actually exists. Rightfully, the debate should have ended with the confirmation of the Aharonov-Bohm experiment.[1–9] Generally, physicists believe it exists, while engineers believe it is a mathematical construct. This can only be resolved through experiment.

Maxwell introduced vector potential after considering arguments by Michael Faraday. Maxwell fully believed in the physical reality of the potential and considered it to be his most important contribution to electromagnetics. This is detailed in Ref. 10.

Heaviside did not believe in potentials. He was the one who cast Maxwell's equations in their familiar **E**, **H**, **D**, **B** form. It is now possible to state Maxwell's equations entirely in terms of the magnetic vector potential $\vec{\mathbf{A}}$, and the electric scalar potential ϕ. Many argue that vector potential is intrinsically unobservable. This paper, then, proposes to right this conceptual wrong.

II. BACKGROUND THEORY

For those who believe in vector potential, the best reference is the paper by E. J. Konopinski,[11] "What the electromagnetic vector potential describes." There he explains that $\vec{A}$ carries linear momentum, equal to $e\vec{A}$, which is a "store" of momentum, which may add (or subtract) from the classical momentum of a free electron immersed in a potential. To indicate that this momentum is available for coupling to electrons, Konopinski calls

$$\vec{P} = m_e \vec{v} + e\vec{A} \tag{1}$$

the "conjugate" momentum. This discrimination is important in that it is the conjugate momentum that must be used in the Schrödinger representation. Likewise, it is $\Delta\vec{P}$ [rather than $\Delta m\vec{v}$] that is the subject of the Heisenberg uncertainty principle when the particle is charged and in an electromagnetic field. From the equation of motion for an electron immersed in a potential, Konopinski shows

$$\frac{d}{dt}[m_e\vec{v} + e\vec{A}] = -\nabla e[\phi - \vec{v}\bullet\vec{A}]. \tag{2}$$

Konopinski calls

$$U = e[\phi - \vec{v}\bullet\vec{A}] \tag{3}$$

the "interaction energy" between charge e and potentials A and ϕ. We are interested in the interaction energy due to A and will therefore drop the ϕ dependence. Clearly, the interaction energy depends on the reference frame used to measure $\vec{v}$ (the electron velocity). In this paper, we will take $\vec{v}$ to be the "drift velocity" of an electron in a plasma tube (in the laboratory). Specifically, we will consider the case when $\vec{v}$ and $\vec{A}$ are collinear.

In Eq. (2), the time derivative of the conjugate momentum (at left) may be considered to be a generalized force acting to accelerate the electron. For $\vec{A}$ of the form

$$\vec{A}(z,t) = \hat{z}\, A\, e^{-j(\omega t - k\bullet z)}, \tag{4}$$

we may evaluate the right hand side of (2). Then, we have

$$\frac{d}{dt}[\vec{P}_{conj}] = e\frac{d}{dz}[\vec{v}_z\bullet\vec{A}_z], \tag{5}$$

$$\frac{d}{dt}[\vec{P}_{conj}] = e\, v_z\, |A|\, e^{-j(\omega t - k\bullet z)}(jk). \tag{6}$$

We multiply by d (the electrode spacing) to obtain ΔP within the tube

$$\Delta P = e\, v_z |A|(jk) d\, e^{-j(\omega t - k\bullet z)}. \tag{7}$$

We now take magnitude P to be ΔP and drop the j

$$P = e\, v_z |A|\, k\, d. \tag{8}$$

In a plasma tube, where v_z is represented by v_{drift}, we may calculate the peak RF oscillatory velocity of the electron

$$v_{rf} = \frac{P}{m_e} = \frac{e\, v_{drift}\, |A|\, k\, d}{m_e}\left[\frac{2\pi}{k\lambda}\right] = \frac{e\, v_{drift}\, |A|\, 2\pi}{m_e}\left(\frac{d}{\lambda}\right), \tag{9}$$

where $2\pi/k\lambda = 1$. This is the peak RF velocity for a single electron in the plasma due to interaction energy with $\vec{A}$. If the plasma electron density is [n], and the plasma cross-sectional area is *Area*, then the macroscopic RF current at frequency ω in the tube is

$$I_{rf} = \left[\frac{e\, v_{drift} A\ 2\pi}{m_e}\right]\left(\frac{d}{\lambda}\right) e\ [n] Area, \tag{10}$$

[a)]Electronic mail: rkzimmerman@gmail.com

 © 2013 AIP Publishing LLC

Downloaded 27 Aug 2013 to 128.183.169.235. This article is copyrighted as indicated in the abstract. Reuse of AIP content is subject to the terms at: http://jap.aip.org/about/rights_and_permissions

where m_e is the electron mass. This is the peak current that may be delivered to an external circuit connected to the electrodes by a transmission line. The available power for a 50 Ω receiver is

$$Available\,Power = \left[\frac{I_{rf}}{\sqrt{2}}\right]^2 50\,\Omega. \tag{11}$$

The $\sqrt{2}$ in the denominator serves to convert the peak RF current to the root mean RMS value.

Often it is desired to express RF power logarithmically with respect to a reference power of 1 milliwatt

$$Available\,Power(dBm) = 10\log(P_{available}) + 30. \tag{12}$$

In the experiment we are about to describe, a frequency of 1300 MHz is used. The drift velocity in the tube is 5.5 km/s for a DC bias current of 8.8 mA. The RF velocity will add and subtract from the drift velocity, serving to redistribute the laminar current flow into charge "bunches" moving at a mean velocity of v_{drift}. It is the DC bias current, provided by the tube power supply, which pushes these charge bunches through the external 50 Ω circuit (the receiver) resulting in 1300 MHz received power. The available power is not the delivered power. This is because the bulb is a high impedance device and has a large mismatch loss driving the 50 Ω cable. The bulb has a voltage drop of 75 volts for a bias current of 8.8 mA. Accordingly, the bulb impedance is

$$Z = \frac{75\text{V}}{8.8\text{mA}} = 8522\,\Omega \tag{13}$$

For a 50 Ω cable, the voltage reflection coefficient is

$$\Gamma = \frac{50-8522}{50+8522} = -0.9885 \tag{14}$$

The RF voltage across the tube will be reduced by a factor of $(1+\Gamma) = 1-0.9885 = 0.0115$. The bulb is a device, and not a transmission line. Accordingly, if the RF voltage is reduced by $(1+\Gamma)$, so will the RF current (this is Ohm's Law). $20\log(0.0115) = -38.8$ dB. There is a second loss term also: The power coupled across the mismatch between the bulb and the coaxial cable is reduced $(1-\Gamma^2)$. $10\log(1-\Gamma^2) = -16.3$ dB. Combining these two terms,

$$P_{delivered} = P_{available} - 55.1\,\text{dB} \tag{15}$$

This detection technique has an analog in an old-fashioned analog telephone. Voice pressure on the microphone modulates the constant carrier line current, causing charge bunches. All the charge is returned to the central office, but with an audio AC component.

There is an exact analog with the electron velocity modulation, which occurs in klystron tubes.

III. EXPERIMENTAL THEORY

In this experiment, a longitudinal vector potential is radiated off the end of a monopole (or dipole) according to the defining relation

$$A(r,t) = \frac{\mu_o}{4\pi}\int_{\Omega}\frac{J(r',t_r)\,e^{-j(\omega t - k\cdot r)}}{|r-r'|}d^3r', \tag{16}$$

where the integral is over the volume Ω containing the current distribution J. This definition is consistent with the Lorentz gauge

$$\nabla\bullet\vec{A} = -\mu_o\varepsilon_o\frac{\partial\phi}{\partial t} = -\left(\frac{1}{c^2}\right)\frac{\partial\phi}{\partial t}, \tag{17}$$

where ϕ is the electric scalar potential. This supports wave propagation at velocity c. Every gauge has a proper velocity associated with it. Only the Lorentz gauge provides propagation at c. Accordingly, only the Lorentz gauge is a physical gauge for vector potential measurements.

Vector potential radiation carries no energy (it is carried by virtual photons). These particles only carry linear momentum.

It is possible to radiate longitudinal $\vec{A}$ without coincident radiation of RF power as detailed by the author in Ref. 12. This technique uses a driven longitudinal probe in a circular waveguide above cutoff for the TM01 mode.

IV. EXPERIMENTAL ARRANGEMENT

The experimental arrangement is depicted in Figure 1. The transmitting monopole is shown in Figure 2, and is centered at 1300 MHz. The receiving neon bulb is shown in Figure 3. The electrodes in the bulb must be oriented such that $\vec{A}$ bridges the gap between the electrodes. In this manner, the electron drift velocity is collinear with $\vec{A}$ longitudinal. A bias current of ±8.8 mA is used. The terminals of the bulb are soldered directly to a coaxial connector, which leads to a 50 Ω transmission line as in Figures 1 and 3. The bias current is supplied to the bulb by the coaxial cable using a commercial in-line bias-tee. The bias-tee has a measured insertion loss of 0.04 dB, and provides an RF isolation to the bias port of better than 25 dB.

The monopole is configured horizontally, with the probe centerline aimed directly at the detector 2 m away.

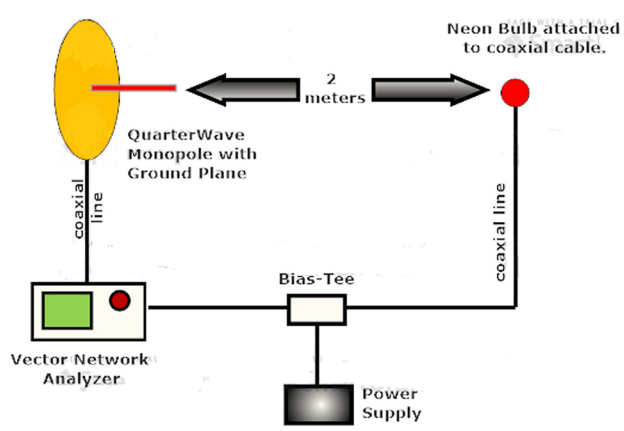

FIG. 1. Experimental arrangement for the reception of longitudinal vector potential radiation with an NE-2 neon bulb. The power supply contains a double-pole double-throw (DPDT) current reversing switch as well as a 16 kΩ current limiting resistor. The power supply consists of (24) 9 V batteries snapped together in series.

Downloaded 27 Aug 2013 to 128.183.169.235. This article is copyrighted as indicated in the abstract. Reuse of AIP content is subject to the terms at: http://jap.aip.org/about/rights_and_permissions

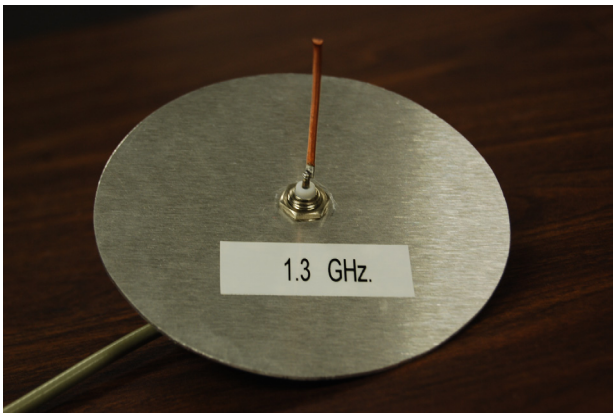

FIG. 2. Photograph of the transmitting monopole. The driven element is a quarter wave long at 1.3 GHz. The radius of the reflector is also a quarter wave at 1.3 GHz. As discussed in Appendix B, the reflector serves to double the magnitude of the forward radiated vector potential A_z.

The electron drift velocity may be calculated from current continuity in the bulb. The relation is as follows:

$$I_{bias} = v_{drift}\ [n]\, e\, Area, \tag{18}$$

where $[n]$ is the electron density, e is the electron charge, and $Area$ is the cross-sectional area of the current carrying plasma. The electron density for NE-2 neon bulbs is 10^{18} electrons per cubic meter. The cross sectional-area is approximately 10^{-5} m^2.

The monopole is driven with 1 mW of RF power (0 dBm). With this power level as a reference, the network analyzer display may be read directly in dBm. This is shown in Figure 4, where the mean received power is −52 dBm. The network analyzer can also display the phase of the received signal relative to the transmitted signal. This is shown in Figure 5 for both positive and negative bias current of 8.8 mA. The RF phase clearly reverses for bias current reversal. This is a cardinal sign of vector potential detection and cannot occur for reception of normal radio waves. The physical theory presented in this paper predicts the actual received RF signal to within ±1.5 dB. If further experiments with different bulbs do not reflect this, the first variable to doubt is $[n]$, the electron density. Usually, the electron density is known only through a literature search.

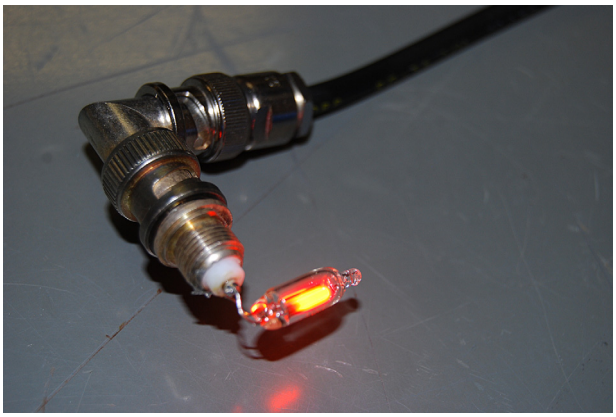

FIG. 3. Photo of the NE-2 neon bulb detector for longitudinal magnetic vector potential.

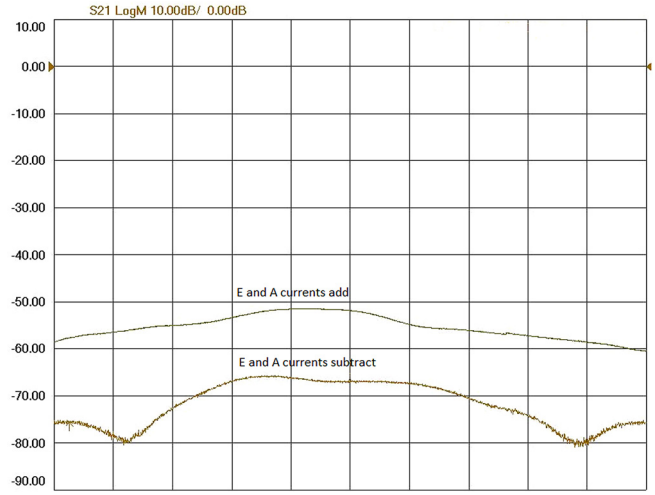

FIG. 4. These two curves show S21 for reversal of the bulb bias current of 8.8 mA. The delta at center frequency is >10 dB. The phase of the vector potential current reverses for reversal of the bias current, as shown in Figure 5. However, at 2 m range, there is also a 1300 MHz longitudinal E field that is received. The E field signal does not change phase upon bias current reversal. Accordingly, for the first bias current (at top), the E current and A current add in phase. For the reversed bias, at bottom, the two currents subtract. E longitudinal is a localized non-propagating field which falls off with distance as $1/R^2$. Only one reflecting plane was used in this experiment (with the monopole).

As a final test for this paper, a gain antenna was examined and tested. The antenna is shown in Figure 6, where the neon bulb is placed a quarter-wave in front of a planar reflector. The antenna works in the following manner: As before, the bulb detects RF current for the forward propagating wave. The wave then reflects from the reflector, so that it reaches the bulb again after a 180° phase delay. However, the direction of propagation is also reversed. For a longitudinal wave, there will be equal detected currents for the forward and reverse waves. The RF current is doubled, resulting in a 6 dB improvement in the received power. This is shown in Figure 7. The calculated antenna pattern is

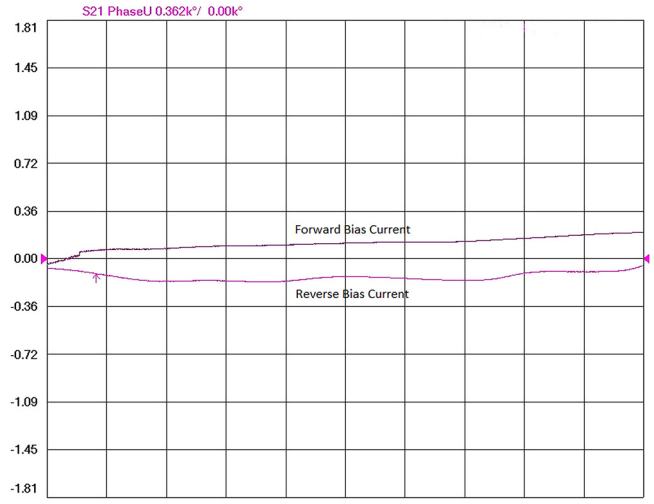

FIG. 5. Network analyzer plot showing RF phase reversal upon reversal of the DC bulb bias current. The vertical scale is 360 degrees per division. The bulb bias current is ±8.8 mA. To "unwind" the phase, a port extension of 73 ns is used on Port 1. The center frequency is 1300 MHz, and the span is 50 MHz.

Downloaded 27 Aug 2013 to 128.183.169.235. This article is copyrighted as indicated in the abstract. Reuse of AIP content is subject to the terms at: http://jap.aip.org/about/rights_and_permissions

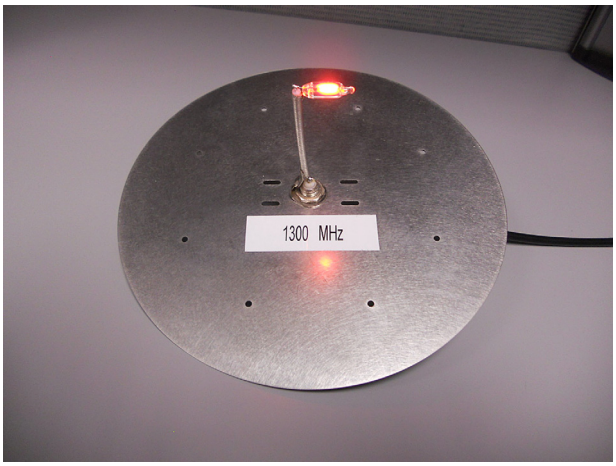

FIG. 6. Photograph of gain antenna for reception. The NE-2 neon bulb is mounted a quarter-wave in front of a planar reflector. This results in a gain of 6 dB, which is shown in Figure 7.

presented in Figures 8(a) and 8(b). The lobe full-width at half-maximum is 76°.

V. DISCUSSION

Detection of longitudinal vector potential radiation with a DC biased neon bulb has been demonstrated.

This experiment demonstrates an entirely new form of radiation—longitudinal magnetic vector potential radiation. These waves display new features: the received phase shows reversal upon detector bias current reversal (unlike TEM radio waves), the waves are longitudinal (unlike TEM radio waves), and the received power comes directly from the receiver power supply.

This provides the means of a new type of electromagnetic communication. Signals may be received "off the end" of a monopole or dipole in the RF null of the transmitting antenna. This may generally be described as a macroscopic Aharonov-Bohm effect: the electron momentum is changed by the time-dependent vector potential much as is demonstrated by the Aharonov-Bohm experiment for a DC (0 Hz.)

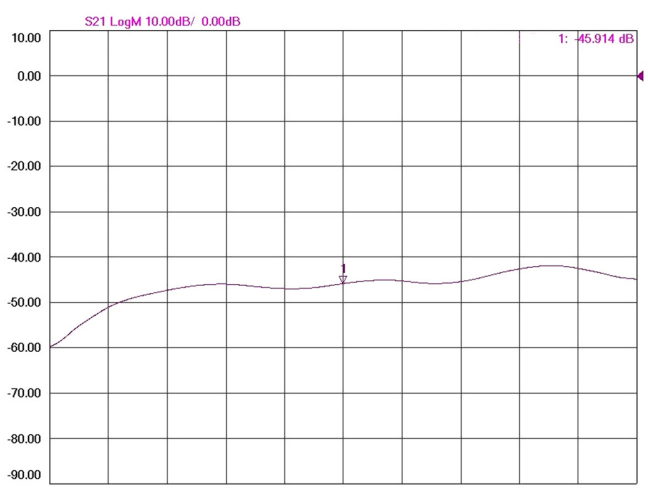

FIG. 7. Vector network analyzer plot showing S21 for the gain antenna. Compare with Figure 4 where the experimental conditions are the same, except now a reflector plane is used behind the NE-2 bulb resulting in a 6 dB signal improvement.

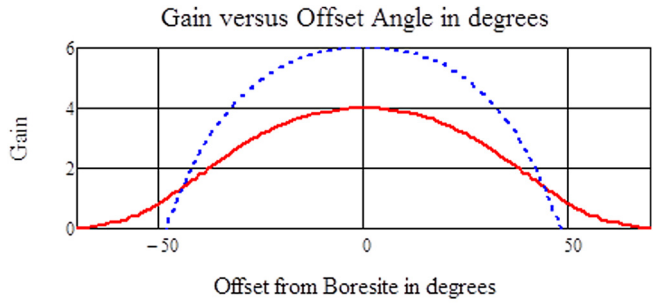

(a)

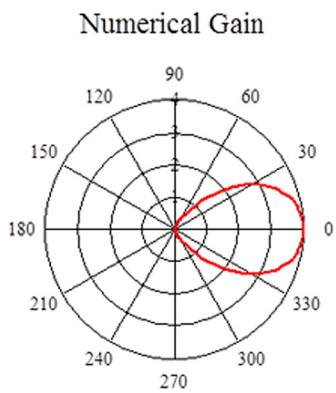

(b)

FIG. 8. (a) Calculated gain pattern of the receiving gain antenna. The dashed curve is in decibels. The solid curve is numerical gain. The full-width at half-max is 76°. (b) Calculated gain polar plot for the receiving gain antenna. The vertical axis is labeled in numerical gain.

vector potential. The most astonishing feature is the detected power does *not* originate at the transmitting antenna; the detected power comes from the detector power supply at the receiver. This is a great advantage for broadcasting, where often immense powers are used at the transmitting site (kW or even MW).

Finally, we assert that the Lorentz gauge is the *only* physical gauge for observing vector potential radiation. Other gauges are mathematical manipulations that result in a velocity of propagation different from c; this is untenable… they must be dismissed as unphysical.

Figure 9 shows the theoretical received signal level versus distance. Signal levels were confirmed for R = 2, 50, and 100 meters. The agreement with theory is excellent.

This experiment provides solid evidence for the existence of vector potential radiation (as predicted by Maxwell and conversely to Heaviside), as well as the possibility to detect such radiation. Appendix A gives Maxwell's equations in terms of $\vec{A}$ and ϕ. Appendix B discusses the use of planar reflectors in this experiment for the transmitting and receiving antennas.

Patent Notice: This detection technology is addressed by U.S. patent 8,165,531. Additional information is available from the patent holder: McMaster University (Hamilton, Ontario). Please contact McMaster Industry Liaison Office, Mr. Paul Grunthal, milo.mcmaster.ca. Phone: (905) 525-9140, ext. 26548.

Downloaded 27 Aug 2013 to 128.183.169.235. This article is copyrighted as indicated in the abstract. Reuse of AIP content is subject to the terms at: http://jap.aip.org/about/rights_and_permissions

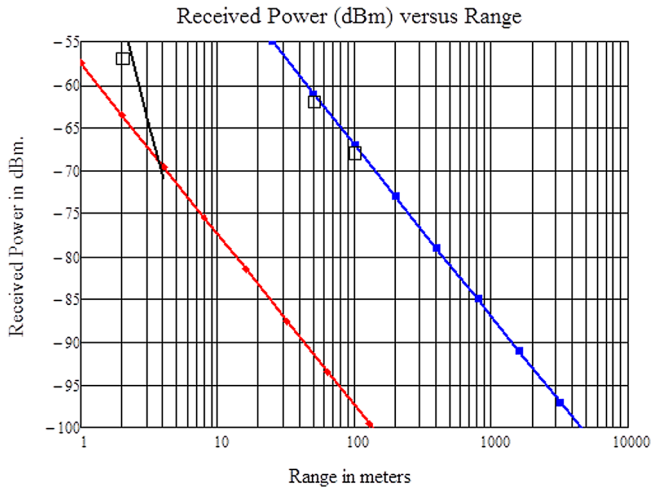

FIG. 9. Plot of theoretical received power for 1 mW and 1 Watt drive to a monopole antenna versus range in meters (log scale). The values are calculated with the theory presented in this paper. The received power at 2, 50, and 100 m has been confirmed experimentally in this work. These points are shown as squares above and are accurate to better than 2 dB. The signal decreases 6 dB for each doubling of range; the markers are spaced for every doubling of range. The top trace is for 1 W RF drive; the lower trace is for 1 mW RF drive. The detector bias current is taken as 8.8 mA. Note that for ranges of 4 m and less, the trace bifurcates, as the current due to **E** longitudinal adds to the current due to **A** longitudinal (for one bias polarity). This yields a power greater than that due to **A** longitudinal alone as is demonstrated in Figure 4.

APPENDIX A: MAXWELL'S EQUATIONS

If $\vec{A}$ and ϕ are expressed in the Lorentz gauge as per the defining relations

$$\mathbf{A}(\mathbf{r},t) = \frac{\mu_o}{4\pi}\int_{\Omega}\frac{\mathbf{J}(\mathbf{r}',t_r)}{|\mathbf{r}-\mathbf{r}'|}d^3\mathbf{r}', \tag{A1}$$

$$\phi(\mathbf{r},t) = \frac{1}{4\,\pi\,\varepsilon_0}\int_{\Omega}\frac{\rho(\mathbf{r}',t_r)}{|\mathbf{r}-\mathbf{r}'|}d^3\mathbf{r}'. \tag{A2}$$

Then, Maxwell's equations may be compactly written as

$$\nabla^2\phi - \frac{1}{c^2}\frac{\partial^2\phi}{\partial t^2} = -\ \frac{\rho}{\varepsilon_0}, \tag{A3}$$

$$\nabla^2\mathbf{A} - \frac{1}{c^2}\frac{\partial^2\mathbf{A}}{\partial t^2} = -\mu_0\mathbf{J}. \tag{A4}$$

These expressions are taken from R. P. Feynman, R. B. Leighton, and M. Sands, *The Feynman Lectures on Physics*, Vol. 2. (Addison-Wesley, 1964).

APPENDIX B: ON THE USE OF REFLECTING SURFACES IN THIS EXPERIMENT

If $\vec{\mathbf{A}}$ is normally incident on a conducting surface, the reflection coefficient is

$$\Gamma_{\text{normal}} = +1, \tag{B1}$$

Also, the direction of propagation will be reversed. Likewise, if $\vec{\mathbf{A}}$ is tangentially incident on a conducting surface, the reflection coefficient is

$$\Gamma_{\text{tangential}} = -1. \tag{B2}$$

These coefficients may be found in most graduate electromagnetic texts.

Accordingly, if a reflecting plane is used with the monopole transmitting antenna, the forward radiated $\vec{\mathbf{A}}$ will be doubled. If a reflector is also used for the receiving antenna, as in Figure 6, we have another factor of 2. These factors will result in a 12 dB enhancement in the received signal level.

[1]Y. Aharonov and D. Bohm, Phys. Rev. **115**, 485 (1959).
[2]R. G. Chambers, Phys. Rev. Lett. **5**, 3 (1960).
[3]H. Boersch, H. Hamisch, D. Wohlleben, and K. Grohmann, Z. Phys. **159**, 397 (1960).
[4]A. Tonomura, N. Osakabe, T. Matsuda, T. Kawasaki, and J. Endo, Phys. Rev. Lett. **56**, 792 (1986).
[5]M. Peshkin and A. Tonomura, *The Aharonov–Bohm Effect, Lecture Notes in Physics* (Springer-Verlag, Berlin, 1989), Vol. 340.
[6]B. E. Allman, A. Cimmino, A. G. Klein, and G. I. Opat, Phys. Rev. Lett. **68**, 2409 (1992).
[7]W. A. Little and R. Parks, Phys. Rev. A **133**, 2820 (1964).
[8]R. A. Webb, S. Washburn, C. P. Umbach, and R. B. Laibowitz, Phys. Rev. Lett. **54**, 2696 (1985).
[9]H. Batelaan and A. Tonomura, Phys. Today **62**(9), 38 (2009).
[10]A. M. Bork, *Maxwell and the Vector Potential, Isis* (The University of Chicago Press for the History of Science Society, 1967), pp. 210–222.
[11]E. J. Konopinski, "What the electromagnetic vector potential describes," Am. J. Phys. **46**, 499–502 (1978).
[12]R. K. Zimmerman, Jr., "Macroscopic Aharonov-Bohm effect at l-band microwave frequencies," Mod. Phys. Lett. B **25**(9), 649–662 (2011).

Downloaded 27 Aug 2013 to 128.183.169.235. This article is copyrighted as indicated in the abstract. Reuse of AIP content is subject to the terms at: http://jap.aip.org/about/rights_and_permissions